

Further Enhancement of the Second-Order Nonlinear Optical (NLO) Coefficient and the Stability of NLO Polymers that Contain Isolation Chromophore Moieties by Using the “Suitable Isolation Group” Concept and the Ar/Ar^F Self-Assembly Effect

Wenbo Wu,^[a] Cheng Ye,^[b] Jingui Qin,^[a] and Zhen Li*^[a]

Abstract: For the first time, a series of second-order NLO poly(arylene-ethynylene)s, in which an isolation chromophore was introduced to enhance the NLO coefficients, were successfully designed and synthesized. Thanks to the isolation chromophore, these polymers demonstrated good NLO activities and optical transparency. To further improve the comprehensive performance of the polymers, different isolation groups of various sizes were introduced

to subtly modify the structure of the polymers according to the “suitable isolation group” concept. The naphthalene (Np) group was found to be a “suitable isolation group” in this series of polymers and polymer **P3** demonstrated the highest d_{33} value

(122.1 pmV⁻¹) of these five polymers. Interestingly, polymer **P5**, which contained a pentafluorophenyl ring as an isolation group, exhibited a much higher NLO effect and stability than polymer **P2**, which just contained normal phenyl rings as isolation groups (97.2 versus 62.5 pmV⁻¹), thus indicating the advantages of the Ar–Ar^F self-assembly effect in the field of nonlinear optics.

Keywords: chromophores · nonlinear optics · polymers · self-assembly · transparency

Introduction

Second-order nonlinear optical (NLO) materials have been extensively studied in recent years because of their potential applications in, for example, ultrafast optical switches, high-speed optical modulators, and high-density optical data storage. Unlike inorganic crystal materials, NLO polymers possess many advantages, such as light weight, low cost, ultrafast response, wide response waveband, high optical-damage threshold, and good processability.^[1] To exhibit an active NLO effect, the macroscopic arrangement of the dipoles of NLO chromophores, which usually possess a donor– π –acceptor (D– π –A) structure with large μ values, should be noncentrosymmetric (typically achieved by using the poling procedure; see the Supporting Information, Chart S1).^[2]

However, the strong intermolecular dipole–dipole interactions within these D– π –A structures typically make the poling-induced noncentrosymmetric alignment of the chromophores a daunting task. Thus, the major problem in NLO research is how to efficiently translate the large β values of the organic chromophores into high macroscopic NLO activities of the corresponding polymers.^[3] In an attempt to partially solve this challenge, since 2006, based on the excellent work reported in the literature^[4] and according to the site-isolation principle proposed by Dalton et al.,^[5] we have been investigating the preparation of different kinds of NLO polymers, in which the size of the isolation groups in the NLO chromophore moieties was changed from small to large and the obtained experimental results demonstrated that the macroscopic nonlinearity of the NLO polymers could be boosted several times by employing a “suitable isolation group” on the NLO chromophore moieties (for selected examples, see the Supporting Information, Charts S2–S6).^[6,7] Based on these experimental results, as well as theoretical analysis, we proposed a new concept in the field of NLO, that is, the “suitable isolation group” concept, which states that, for a given chromophore moiety and a given linkage position, there should be a suitable isolation group present to boost its microscopic β value in order to afford higher macroscopic NLO activities.

However, in all of the previous work in this area, the isolation groups were non-polar groups that were designed to impede the strong interactions between the chromophore moieties. Moreover, they did not directly contribute to the macroscopic NLO effect, but rather decreased the effective

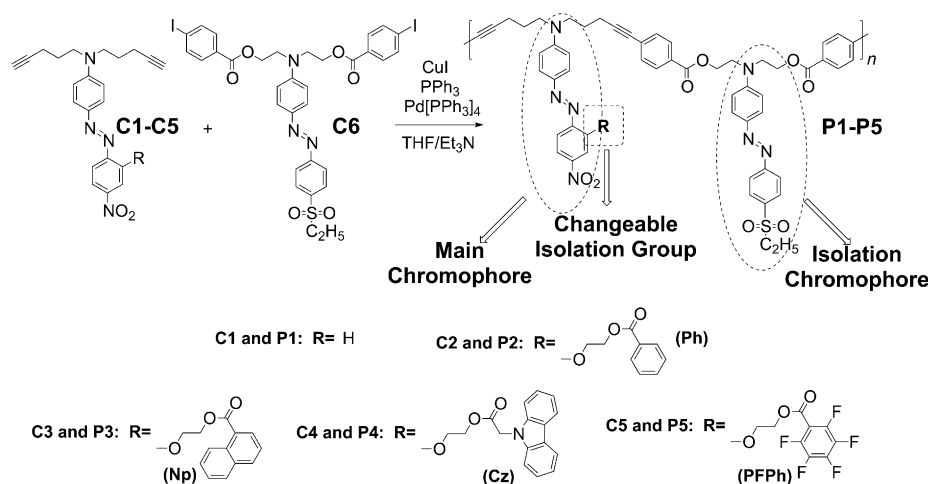
[a] W. Wu, Prof. J. Qin, Prof. Z. Li

Department of Chemistry, Hubei Key Laboratory of Organic and Polymeric Optoelectronic Materials
Wuhan University
Wuhan 430072 (China)
Fax: (+86)27-68756757
E-mail: lizhen@whu.edu.cn
lichemlab@163.com

[b] Prof. C. Ye

Organic Solids Laboratories
Institute of Chemistry, Chinese Academy of Sciences
Beijing 100080 (China)

Supporting information for this article is available on the WWW under <http://dx.doi.org/10.1002/asia.201300010>.



Scheme 2. Synthesis of NLO polymers **P1–P5**.

fluoroaromatic dendron-substituted NLO chromophores that formed through complementary $\text{Ar}-\text{Ar}^{\text{F}}$ interactions, Jen and co-workers developed a new class of molecular glass (see the Supporting Information, Chart S9) that exhibited an improved poling efficiency and a much enhanced macroscopic NLO effect,^[10] owing to the reversible $\text{Ar}/\text{Ar}^{\text{F}}$ self-assembly effect, which helped to align the chromophores (see the Supporting Information, Chart S10). In 2012, we employed these $\text{Ar}-\text{Ar}^{\text{F}}$ interactions to improve the NLO coefficients of polymers (see the Supporting Information, Chart S11), as well as dendrimers and hyperbranched polymers.^[11] We used perfluorophenyl rings rather than phenyl rings as the isolation group (polymer **P5**, Scheme 2) to further investigate whether these $\text{Ar}-\text{Ar}^{\text{F}}$ interactions could be used in NLO polymers that contained isolation groups and the results were encouraging: Polymer **P5** exhibited a much higher d_{33} value (up to 97.2 pm V^{-1}) and better stability than its analogue with normal isolation groups (polymer **P2**). Herein, we report the synthesis, characterization, and properties of these polymers (**P1–P5**) in detail.

Results and Discussion

Structural Characterizations and Self-Assembly Effect

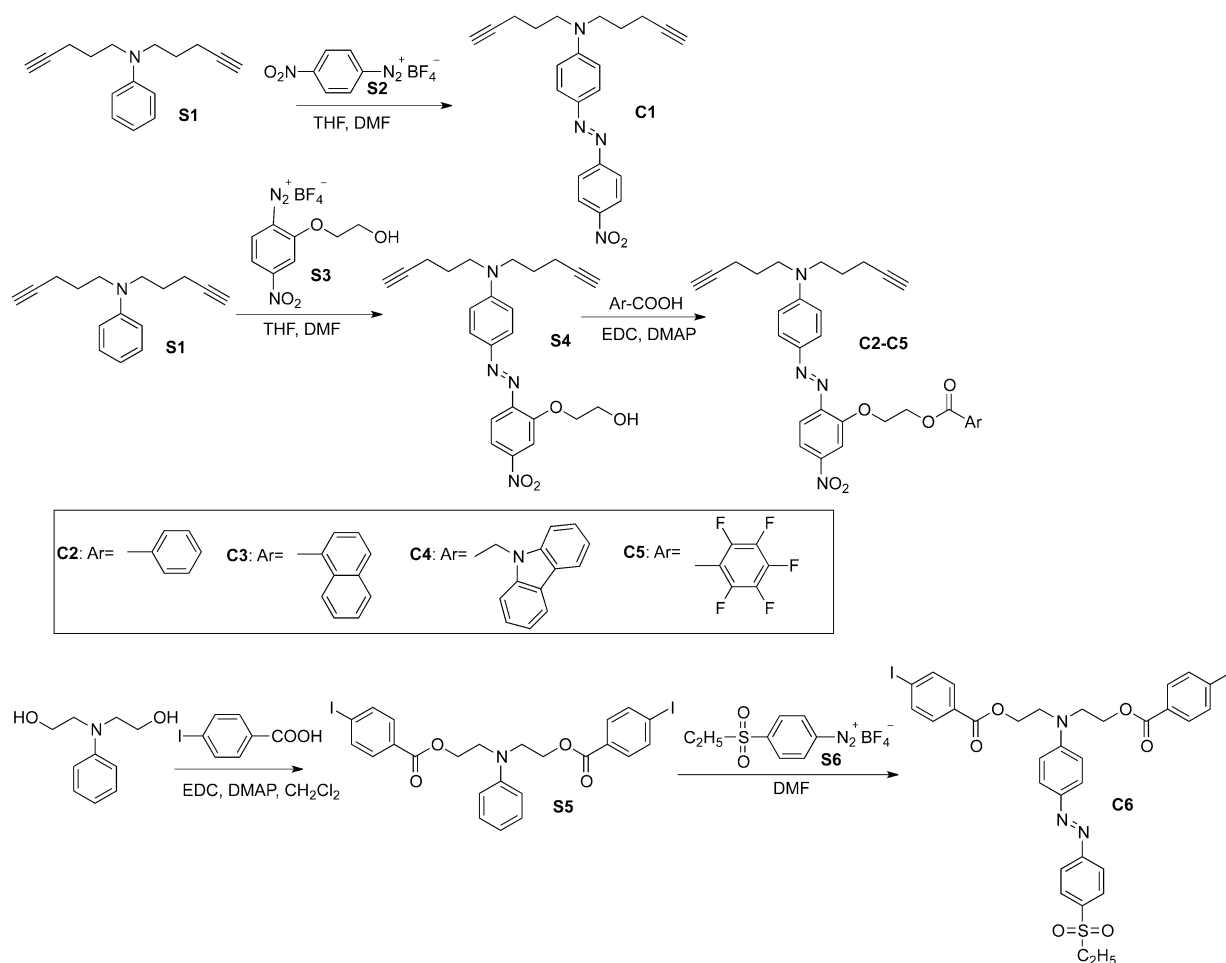
The syntheses of polymers **P1–P5** and monomers **C1–C6** are presented in Scheme 2 and Scheme 3, respectively. These synthetic routes are only comprised of simple reactions, such as azo-coupling, esterification, and Sonogashira coupling reactions. The as-obtained polymers were readily soluble in common polar organic solvents, such as CH_2Cl_2 , CHCl_3 , THF, *N,N*-dimethylformamide (DMF), and dimethyl sulfoxide (DMSO); this was convenient for testing their NLO (and other) properties.

The obtained polymers were characterized by spectroscopic methods and they all gave satisfactory spectroscopic data (for detailed analytical data, see the Experimental Sec-

tion and the Supporting Information). The Supporting Information, Figure S1, shows the FTIR spectra of polymers **P1–P5**, in which the absorption bands that are associated with the nitro, sulfonyl, and carbonyl groups are present at about 1338 , 1517 , and 1138 and 1720 cm^{-1} , respectively, thus indicating that the chromophore and isolation groups are stable during the Sonogashira polymerization reactions. At the same time, the absorption band that was derived from the $\text{C}-\text{H}$ stretching vibrations at about 3277 cm^{-1} disappeared in the spectra of polymers **P1–P5**,

whilst the $\text{C}\equiv\text{C}$ stretching vibrations (at about 2100 cm^{-1}) were still present, thus indicating that the polymerization reactions were successful.

NMR spectroscopy is an especially useful tool for determining the structures of polymers. As an example, the ^1H NMR spectra of polymer **P2** and its corresponding chromophores (**C2** and **C6**) in CDCl_3 are shown in Figure 1; the other spectra are provided in the Supporting Information, Figures S2–S9. The chemical shifts were consistent with the proposed structures, as shown in Scheme 2 and Scheme 3, although some signal broadening was observed in the spectrum of polymer **P2**, owing to the polymerization. In the ^1H NMR spectrum of polymer **P5**, which contained pentafluorophenyl rings (Figure 2, the chemical shifts of the protons adjacent to the pentafluorobenzoic group (COOCH_2) shifted a little towards higher field ($\delta \approx 4.80 \text{ ppm}$) in comparison with the spectrum of chromophore **C5** ($\delta \approx 4.88 \text{ ppm}$), thus indicating that the electron-withdrawing activity of the pentafluorobenzoic group had become weaker and that the electron-density distribution of the perfluoroaromatic rings had become higher. There is only one possible reason for this phenomenon, that is, that the self-assembly effect between the perfluoroaromatic rings and the aromatic rings in the polymer increased the electron-density distribution of the perfluoroaromatic rings. However, there were three more phenyl rings in polymer **P5** than in monomer **C5** and, thus, it was very important to confirm which of these could form interactions with the pentafluorophenyl rings. Therefore, two model polymers, **PM1** and **PM2** (see the Supporting Information, Scheme S1), were also prepared. In comparison with polymer **P5**, there were no isolation chromophores in polymer **PM1** and the phenyl rings in the main chain were replaced by triazole rings in polymer **PM2**. As shown in Figure 3, the resonance of the methylene protons that were linked to the ester groups (COOCH_2) in the ^1H NMR spectrum of polymer **PM2** was not shifted compared to the corresponding signal in the spectrum of chromophore **C5**, whereas it was shifted slightly towards



Scheme 3. Synthesis of monomers C1–C6.

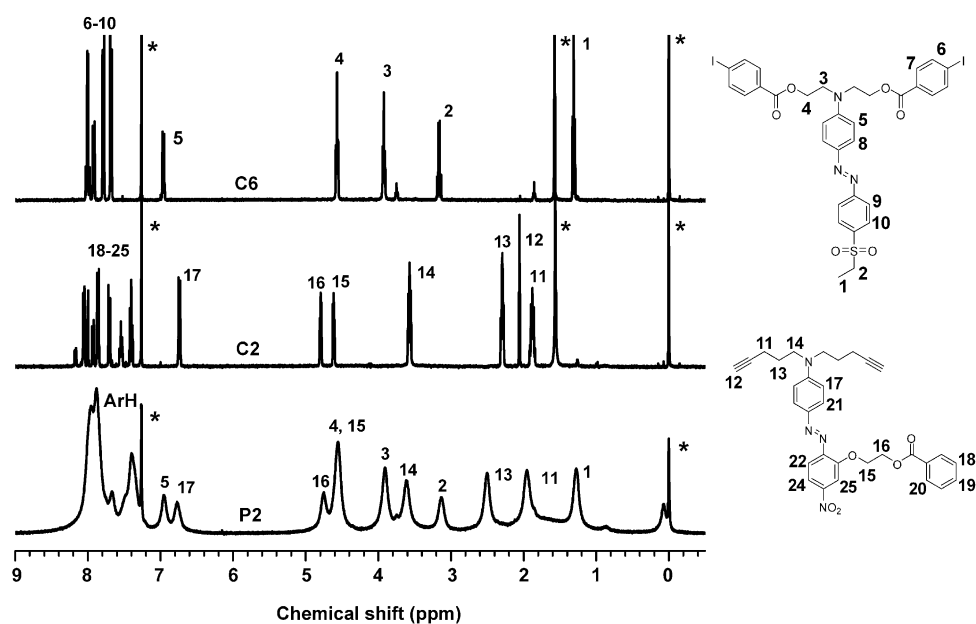


Figure 1. ¹H NMR spectra of polymer P2 and its corresponding chromophores in CDCl₃; the solvent peaks and the peak for TMS are marked with asterisks (*).

higher field in polymer **PM1**, very similar to the results for polymer **P5**. According to this phenomenon, a preliminary conclusion could be reached, that is, in this case, a Ar–Ar^F self-assembly effect is present between the isolation groups and the polymer main chains.

On the other hand, owing to there being three types of F atoms in the pentafluorophenyl groups, there should be three peaks in the corresponding ¹⁹F NMR spectrum. However, as shown in Figure 4, along with the three original peaks, there were some additional peaks in the ¹⁹F NMR spectra of polymers **P5** and **PM1**. This result is presumably owing to the strong Ar–Ar^F self-assembly effect, which may change the environ-

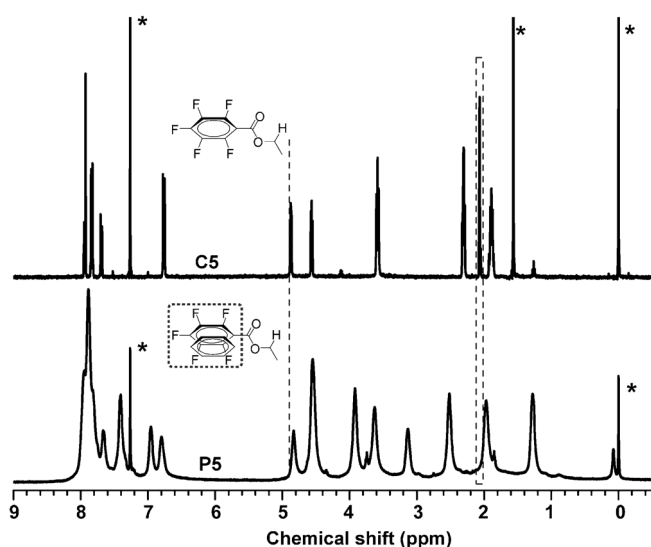


Figure 2. ^1H NMR spectra of polymer **P5** and its corresponding chromophore in CDCl_3 ; the solvent peaks and the peak for TMS are marked with asterisks (*).

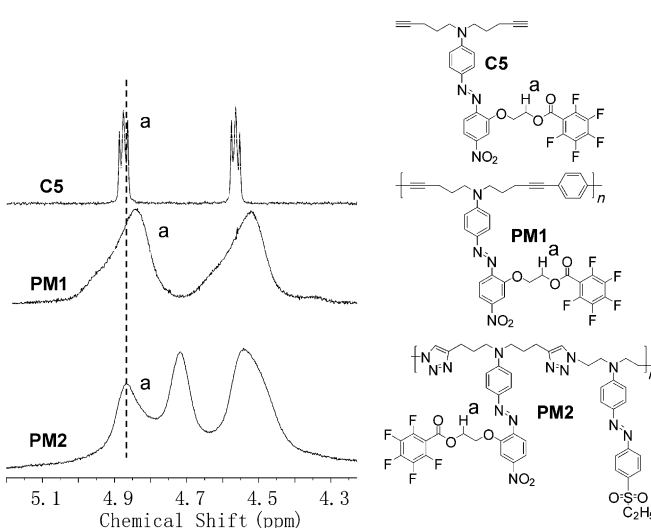


Figure 3. Structures of model polymers **PM1** and **PM2** and their ^1H NMR spectra.

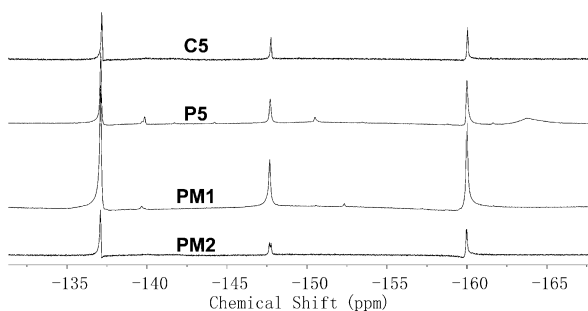


Figure 4. ^{19}F NMR spectra of the polymers and chromophore that contained perfluoroaromatic rings as isolation groups.

ment around some of the F atoms. This phenomenon is consistent with the results of the ^1H NMR analysis, that is, that strong $\text{Ar}-\text{Ar}^{\text{F}}$ interactions exist between the isolation groups and the polymer main chains.

The molecular weights of the polymers were determined by gel-permeation chromatography (GPC) with THF as an eluent and polystyrene as calibration standards. As shown in Table 1 and the Experimental Section, the molecular

Table 1. Characterization data of the polymers.

	Yield [%]	M_w [a]	M_w/M_n [a]	T_g [b] [°C]	T_d [c] [°C]
P1	73.8	9900	1.76	134	268
P2	83.3	12900	1.56	131	284
P3	89.3	13200	1.70	142	262
P4	89.1	14900	1.99	135	269
P5	79.8	13800	1.61	161	231

[a] Determined by GPC in THF, based on calibration with polystyrene; [b] glass-transition temperature of the polymers, as determined by DSC analysis under an argon atmosphere at a heating rate of $10^\circ\text{C min}^{-1}$; [c] 5% weight-loss temperature of the polymers, as determined by TGA under a nitrogen atmosphere at a heating rate of $10^\circ\text{C min}^{-1}$.

weights of the polymers were within the range 9900–14900 and the increasing trend in the tested GPC results was consistent with the increase in the molecular weight of the corresponding nitro-based chromophores. The thermal behavior of these polymers was studied by thermogravimetric analysis (TGA) and by differential scanning calorimetry (DSC) under a nitrogen atmosphere. As shown in Table 1 and the Supporting Information, Figure S10, all of the polymers exhibited similar 5% weight-loss temperatures (T_d) and glass-transition temperatures (T_g), owing to their similar chemical structures, except for polymer **P5**. In this case, because its pentafluorophenyl groups were not so stable, polymer **P5** exhibited the lowest T_d value. However, the T_g value of polymer **P5** (161°C) was much higher than those of the other polymers, owing to the self-assembly effect between the phenyl and pentafluorophenyl rings, similar to our previous work.^[11] Furthermore, considering that the stability of the NLO effect is associated with the glass-transition temperature, this higher T_g value should be beneficial for its practical applications.

UV/Vis Spectra and Effects of the Isolation Chromophores

The UV/Vis absorption spectra of these polymers in different solvents are shown in Figure 5 and the Supporting Information, S11–S15, whereas the maximum absorption wavelengths for the $\pi-\pi^*$ transition of the azo moieties are shown in Table 2. All of the polymers showed similar λ_{max} values in the same solvent (Figure 5 A shows the UV/Vis absorption spectra in THF, as an example), thus indicating that the introduction of isolation groups of different sizes, including pentafluorophenyl groups, almost showed no effect on the $\mu\beta$ value of the NLO chromophore, which could allow for a comparison of their NLO properties at the same level.

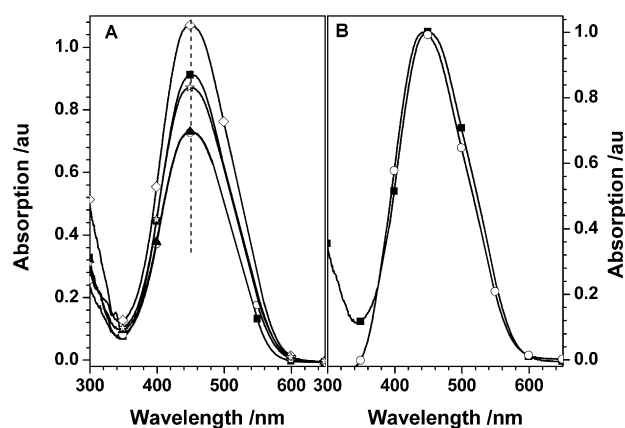


Figure 5. A) UV/Vis spectra of polymers **P1** (■), **P2** (○), **P3** (▲), **P4** (◇), and **P5** (☆) in THF (0.02 mg mL⁻¹); B) normalized UV/Vis spectra (as solutions in THF) of polymer **P5** (■) and a mixture of its corresponding chromophores (**C5** and **C6**; (○)).

Table 2. Maximum absorptions of the polymers (λ_{\max} , in nm).^[a]

	THF ^[b]	1,4-Dioxane	CHCl ₃	CH ₂ Cl ₂	DMF	DMSO	Film
P1	449 (444)	447	449	451	467	470	460
P2	448 (445)	442	443	445	463	471	460
P3	450 (441)	442	441	444	464	469	463
P4	451 (442)	443	444	446	462	469	463
P5	449 (442)	443	441	448	465	467	466

[a] The maximum absorption wavelengths of the polymers (chromophore molecules) were determined in solution at a fixed concentration of 0.02 mg mL⁻¹ (2.5 × 10⁻⁵ mol mL⁻¹). [b] The maximum absorption wavelengths of mixtures of the corresponding small chromophore molecules (diluted solutions in THF) are given in parentheses.

On the other hand, this phenomenon also showed that the presence of pentafluorophenyl groups did not influence the electronic behavior of the chromophore moieties, thus indicating that there were no interactions between the phenyl rings in the chromophore and the pentafluorophenyl rings. Thus, a self-assembly effect should exist between the pentafluorophenyl isolation groups and the phenyl groups in the polymer main chain, which is consistent with the results from the NMR analysis.

Moreover, to determine the effect of the isolation chromophores on the NLO of the polymers, the UV/Vis spectra of the corresponding chromophores (that is, an equivalent mixture of the nitro- and sulfonyl-based chromophores) were also tested and the results are also listed in Table 2. Similar to our previous work,^[8a] the UV/Vis spectra of the polymers also showed an obvious red-shift in the absorption peak (Figure 6B shows the spectra of polymer **P5** and its corresponding chromophores as an example; for the UV/Vis spectra of the other polymers and chromophores, see the Supporting Information, Figures S16–S19) in comparison with the absorption peaks of their corresponding chromophores. However, until now, the reasons for this red-shift were not clear and further research was still needed.

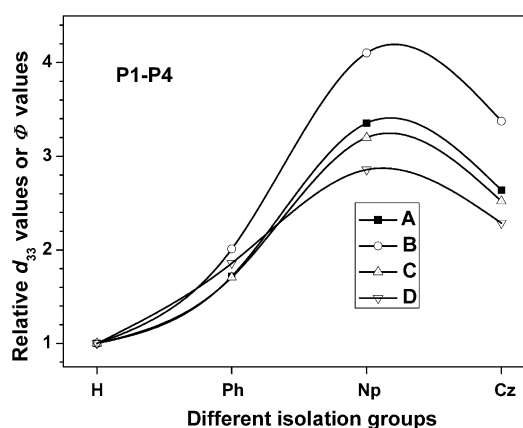


Figure 6. A) Comparison of the d_{33} values of polymers **P1–P4**; B) comparison of the calculated d_{33} values of the polymers, which were obtained from the experimentally determined d_{33} values by dividing the concentrations of the active chromophore moieties in the polymers; C) comparison of the calculated $d_{33}(\infty)$ values of the polymers, according to the approximate two-level model; D) comparison of the Φ values of the polymers. All of these values were determined relative to polymer **P1**.

NLO Properties

In our previous work,^[8] because the isolation chromophore could impede the strong electronic interactions between the main chromophores and because the isolation chromophore itself could directly contribute to the macroscopic NLO effect, the polymers that contained isolation chromophore moieties, including hyperbranched polymers and dendrimers, demonstrated large d_{33} values. Considering that the structures of the polymers investigated herein were modified further, it might also be interesting to investigate their NLO activities; thus, their poled thin films were prepared. The most convenient technique to study second-order NLO activity is to investigate the second harmonic generation (SHG) processes, which are characterized by the SHG coefficient (d_{33}). The method for the calculation of the SHG coefficients of the poled films has been reported previously.^[12] From the experimental data, the d_{33} values of these polymers were calculated at a fundamental wavelength of 1064 nm (Table 3). To check the reproducibility of these results, we repeated the measurements three times.

These NLO results are encouraging and we have clearly shown that the concept of a suitable isolation group could still work in NLO polymers that contain isolation chromophores. According to the concept of a suitable isolation group, for a given chromophore moiety and a given linkage position, there should be a suitable isolation group that could efficiently boost its microscopic $\mu\beta$ value to afford higher macroscopic NLO activities. Thus, we introduced different isolation groups, from small (H) to larger moieties (carbazole, Cz), into the main (nitro-based) chromophore to further adjust its structure. Figure 6A showed a comparison of the d_{33} values of the polymers, by using polymer **P1** (without any isolation groups) as a reference. We found that the d_{33} values did not always increase as the isolation groups became larger and, for this series of polymers, the d_{33} value

that the dipole–dipole interactions become much smaller on the introduction of an isolation chromophore. Furthermore, the d_{33} value of polymer **P3** was at least 40 pm V^{-1} higher than those of NLO polymers that only contained nitro-based chromophore moieties, as shown in Scheme 4, thus further confirming the advantages of isolation chromophores.

To consider the effects of different molar concentrations of the active chromophore moieties in the polymers, we divided the experimentally determined d_{33} values by the molar concentrations of the active chromophores and compared the results with that of polymer **P1** as a reference (Figure 6B). Because there may be some resonance enhancement, owing to the absorption of the chromophore moieties at 532 nm ,^[13] the NLO properties of polymers **P1–P4** ($d_{33}(\infty)$), which were calculated by using the approximate two-level model, should be weaker (Table 3). Moreover, we drew curves by using polymer **P1** as a reference (Figure 6C); clearly, the trends in these curves were the same and, in this system, the naphthalene group was a suitable isolation group, thus confirming our previous idea.

On the other hand, the presence of pentafluorophenyl groups could enhance the NLO activity of a polymer, similar to the work by Jen and co-workers.^[10] Owing to the Ar/Ar^F self-assembly interactions, the poling procedure was slightly different from that of normal chromophores, as proposed by Jen and co-workers (see the Supporting Information, Chart S10), and the reversible Ar/Ar^F self-assembly effect could help the alignment of the chromophores to enhance the NLO effect. In this work, both the d_{33} (97.2 pm V^{-1}) and $d_{33}(\infty)$ values (18.3 pm V^{-1}) of polymer **P5**, which contained pentafluorophenyl groups as isolation groups, were much higher (about 1.5 times) than those of its analogue (polymer **P2**), which just contained phenyl groups as isolation groups, thus indicating that the Ar/Ar^F self-assembly could also enhance the NLO activities of polymers that contained isolation chromophores.

To further study the alignment behavior of the chromophore moieties in the polymers, the order parameter (Φ) of the polymers (Table 3) was also calculated from the change in the UV/Vis spectra of their thin films before and after poling under an electric field, according to the equation described in Table 3, footnote [e]. Figure 7 shows the UV/Vis spectra of films of polymers **P2** and **P5** before and after poling. Clearly, the Φ value of polymer **P5** (0.19) is much higher than that of polymer **P2** (0.13), thus indicating a good alignment of the chromophore moieties in the poled film of polymer **P5** and further confirming the advantages of the self-assembly effect in the NLO polymers. Moreover, the Φ values of the other polymers were also tested (see the Supporting Information, Figures S20–S22). Once again, we drew the curve, still taking polymer **P1** as a reference (Figure 6D), and the trend was similar to the previous results.

The dynamic thermal stabilities of the NLO activities of polymers **P1–P5** were investigated by depoling experiments, in which the real-time decay of their SHG signals was monitored as the poled films were heated from room tempera-

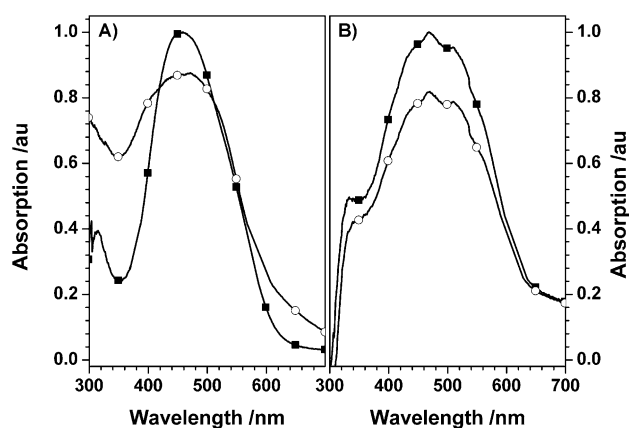


Figure 7. A) Absorption spectra of films of polymers **P2** and B) **P5** before (■) and after (○) poling.

ture to 160°C in air at a heating rate of 4°Cmin^{-1} . As shown in Figure 8, all of the polymers were relatively stable and the onset temperatures for decay in the d_{33} values were

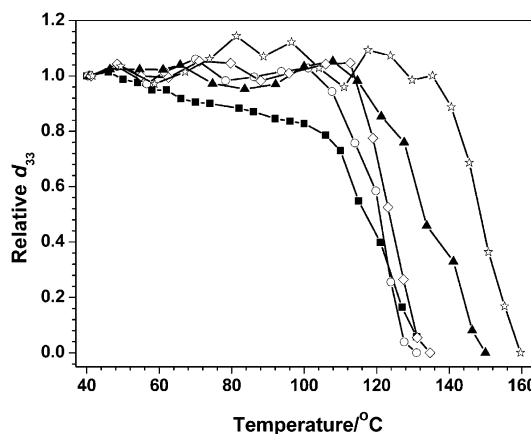


Figure 8. Decay curves of the SHG coefficients of polymers **P1** (■), **P2** (○), **P3** (▲), **P4** (◇), and **P5** (☆) as a function of temperature.

all higher than 100°C . In addition, polymer **P5** showed a much higher onset temperature (141°C) than the other polymers. This result means that, to destroy the alignment of the chromophore moieties in polymer **P5**, much more energy is needed, thus indicating that the Ar–Ar^F self-assembly effect is still present after poling and that these interactions could increase the stability of the NLO polymers, in accordance with the poling procedure proposed by Jen and co-workers (see the Supporting Information, Chart S10).

Conclusions

In summary, a new series of NLO poly(arylene-ethynylene)s that contained isolation chromophore were successfully prepared by employing Sonogashira polymerization reactions. To further improve the comprehensive performance of the

NLO polymers, different isolation groups were introduced to subtly modify the structure of the polymers. Our results showed that this “suitable isolation group” concept could also be applied to isolation-chromophore-containing NLO polymers and polymer **P3**, which contained naphthalene moieties as isolation groups, exhibited the highest d_{33} value and slightly improved stability. On the other hand, thanks to the Ar–Ar^F self-assembly effect, polymer **P5** demonstrated much larger d_{33} values and higher stability than its **P2** analogue, which only contained phenyl rings as isolation groups, thus indicating that the Ar–Ar^F reversible self-assembly effect could help to align the chromophore moieties and enhance the stability of the aligned structure.

Experimental Section

Materials

THF was dried over and distilled from K/Na alloy under a dry nitrogen atmosphere. Triethylamine was distilled under normal pressure and stored over potassium hydroxide. CH₂Cl₂ was dried over CaH₂ and distilled under normal pressure before use. The syntheses of *N,N*-di(4-pentynyl)benzenamine (**S1**)^[14a] and diazonium fluoroborates **S2**,^[8b] **S3**,^[10a] and **S6**^[8b] were reported in our previous work. 2-(9*H*-Carbazol-9-yl)acetic acid was synthesized according to a literature procedure.^[14b] *N*-Phenyldiethanol was bought from Fluka and 4-iodobenzoic acid and pentafluorobenzoic acid were purchased from Alfa-Aesar. All other reagents were used as received.

Instrumentation

¹H NMR spectra were measured on Varian Mercury 300 or Bruker ARX 400 spectrometers by using tetramethylsilane (TMS; $\delta=0$ ppm) as an internal standard. FTIR spectra were recorded on a PerkinElmer-2 spectrometer in the range 3000–400 cm⁻¹. UV/Vis spectra were obtained on a Shimadzu UV-2550 spectrometer. Elemental analysis was performed on a CARLOERBA-1106 microelemental analyzer. Gel-permeation chromatography (GPC) was used to determine the molecular weights of the polymers. GPC analysis was performed on a Waters HPLC system that was equipped with a 2690D separation module and a 2410 refractive index detector. Polystyrene standards were used as calibration standards for GPC, THF was used as an eluent, and the flow rate was 1.0 mL min⁻¹. Thermal analysis was performed on a NETZSCH STA449C thermal analyzer at a heating rate of 10 °C min⁻¹ under a nitrogen atmosphere at a flow rate of 50 cm³ min⁻¹ for the thermogravimetric analysis (TGA) and the thermal transitions of the polymers. The thickness of the films was measured on an Ambios Technology XP-2 profilometer.

General Procedure for the Synthesis of Chromophores **C1** and **S4**

An equimolar mixture of *N,N*-di(4-pentynyl)benzenamine and the diazonium salt was dissolved in THF/DMF (1:1 v/v) at 0 °C. The reaction mixture was stirred for 12 h at 0 °C, treated with water, extracted with CH₂Cl₂, and washed with brine. The organic layer was dried over anhydrous sodium sulfate. After the removal of the organic solvent, the crude product was purified by column chromatography on silica gel.

C1: *N,N*-Di(4-pentynyl)benzenamine (**S1**, 541 mg, 2.40 mmol) and 4-nitrobenzenediazonium fluoroborate (**S2**, 568 mg, 2.40 mmol). The crude product was purified by column chromatography on silica gel (EtOAc/petroleum ether, 1:4 v/v) to afford a deep-red solid (674 mg, 75.1% yield). ¹H NMR (400 MHz, CDCl₃, 298 K): $\delta=1.87$ (m, 4H; CH₂), 2.05 (s, 2H; C≡C–H), 2.29 (m, 4H; CH₂), 3.58 (t, $J=6.0$ Hz, 4H; NCH₂), 6.80 (d, $J=8.0$ Hz, 2H; ArH), 7.90 (m, 4H; ArH), 8.32 ppm (d, $J=8.0$ Hz, 2H; ArH); ¹³C NMR (75 MHz, CDCl₃, 298 K): $\delta=16.6$, 26.2, 50.2, 69.7, 83.7, 111.7, 123.0, 125.2, 126.7, 144.0, 147.5, 151.7, 157.1 ppm; UV/Vis (THF, 1×10^{-5} mmol mL⁻¹): $\lambda_{\max}=482$ nm; IR (thin film): $\tilde{\nu}=3200$ (C≡C–H),

1515, 1337 cm⁻¹ (NO₂); elemental analysis calcd (%) for C₂₂H₂₄N₄O₂: C 70.19, H 6.43, N 14.88; found: C 69.82, H 6.81, N 14.56.

S4: *N,N*-Di(4-pentynyl)benzenamine (**S1**, 901.3 mg, 4.0 mmol) and diazonium salt **S3** (1.19 g, 4.0 mmol). The crude product was purified by column chromatography on silica gel (EtOAc/petroleum ether, 2:1 v/v) to afford a deep-red solid (1.1 g, 63.3% yield). ¹H NMR (400 MHz, CDCl₃, 298 K): $\delta=1.88$ (m, 4H; CH₂), 2.05 (s, 2H; C≡C–H), 2.30 (m, 4H; CH₂), 3.59 (t, $J=6.0$ Hz, 4H; NCH₂), 4.00 (t, $J=4.0$ Hz, 2H; OCH₂), 4.37 (t, $J=4.0$ Hz, 2H; OCH₂), 6.80 (d, $J=8.0$ Hz, 2H; ArH), 7.72 (d, $J=8.0$ Hz, 1H; ArH), 7.86 (d, $J=8.0$ Hz, 2H; ArH) 7.95 ppm (m, 2H; ArH).

General Procedure for the Synthesis of Chromophores **C2–C5**

Chromophore **S4** (1.00 equiv), the carboxy-containing compound (1.50 equiv), 1-(3-dimethylaminopropyl)-3-ethylcarbodiimide hydrochloride (EDC, 2.00 equiv), and 4-dimethylaminopyridine (DMAP, 0.20 equiv) were dissolved in dry CH₂Cl₂ (0.1 mmol mL⁻¹ chromophore **S4**) and the mixture was stirred at RT for 3 h. Then, the mixture was treated with a saturated solution of citric acid, extracted with CH₂Cl₂, and washed with saturated solutions of citric acid and brine. After the removal of the solvent, the crude product was purified by column chromatography on silica gel.

C2: Chromophore **S4** (499.7 mg, 1.15 mmol) and benzoic acid (211.3 mg, 1.73 mmol). The crude product was purified by column chromatography on silica gel (EtOAc/CHCl₃, 1:20 v/v) to afford a deep-red solid (614.3 mg, 99.2% yield). ¹H NMR (400 MHz, CDCl₃, 298 K): $\delta=1.87$ (m, 4H; CH₂), 2.06 (s, 2H; C≡C–H), 2.30 (m, 4H; CH₂), 3.58 (t, $J=8.0$ Hz, 4H; NCH₂), 4.62 (t, $J=4.0$ Hz, 2H; OCH₂), 4.80 (t, $J=4.0$ Hz, 2H; COOCH₂), 6.74 (d, $J=8.0$ Hz, 2H; ArH), 7.40 (t, $J=8.0$ Hz, 2H; ArH), 7.55 (t, $J=8.0$ Hz, 1H; ArH), 7.69 (d, $J=8.0$ Hz, 1H; ArH), 7.86 (d, $J=8.0$ Hz, 1H; ArH), 7.92 (m, 1H; ArH), 8.05 (m, 3H; ArH), 8.17 ppm (d, $J=8.0$ Hz, 1H; ArH); ¹³C NMR (75 MHz, CDCl₃, 298 K): $\delta=49.5$, 61.7, 64.1, 67.9, 101.0, 110.2, 111.6, 117.3, 126.0, 128.7, 130.7, 137.6, 144.8, 147.0, 148.0, 150.7, 154.5, 165.7 ppm; UV/Vis (THF, 1×10^{-5} mmol mL⁻¹): $\lambda_{\max}=489$ nm; IR (KBr): $\tilde{\nu}=3267$ (C≡C–H), 1711 (C=O), 1519, 1335 cm⁻¹ (NO₂); elemental analysis calcd (%) for C₃₁H₃₀N₄O₅: C 69.13, H 5.61, N 10.40; found: C 68.77, H 6.06, N 10.06.

C3: Chromophore **S4** (152 mg, 0.35 mmol) and 1-naphthoic acid (90 mg, 0.525 mmol). The crude product was purified by column chromatography on silica gel (EtOAc/CHCl₃, 1:20 v/v) to afford a deep-red solid (199 mg, 96.6% yield). ¹H NMR (300 MHz, CDCl₃, 298 K): $\delta=1.84$ (m, 4H; CH₂), 2.04 (s, 2H; C≡C–H), 2.27 (brs, 4H; CH₂), 3.53 (brs, 4H; NCH₂), 4.66 (brs, 2H; OCH₂), 4.89 (brs, 2H; COOCH₂), 6.67 (d, $J=8.7$ Hz, 2H; ArH), 7.41 (t, $J=7.5$ Hz, 1H; ArH), 7.53 (t, $J=8.0$ Hz, 2H; ArH), 7.74 (d, $J=8.7$ Hz, 1H; ArH), 7.86 (brs, 3H; ArH), 7.95 (d, $J=8.7$ Hz, 1H; ArH), 8.01 (brs, 2H; ArH), 8.22 (d, $J=6.6$ Hz, 1H; ArH), 8.95 ppm (d, $J=8.1$ Hz, 1H; ArH); ¹³C NMR (75 MHz, CDCl₃, 298 K): $\delta=16.2$, 26.0, 50.1, 63.3, 68.7, 69.8, 83.3, 110.6, 111.6, 117.6, 117.8, 124.8, 126.0, 126.4, 126.6, 126.9, 128.1, 128.7, 130.8, 131.6, 133.7, 133.9, 144.5, 147.7, 148.2, 151.3, 155.0, 167.6 ppm; UV/Vis (THF, 1×10^{-5} mmol mL⁻¹): $\lambda_{\max}=490$ nm; IR (thin film): $\tilde{\nu}=3295$ (C≡C–H), 1716 (C=O), 1514, 1337 cm⁻¹ (NO₂); elemental analysis calcd (%) for C₃₅H₃₂N₄O₅: C 71.41; H 5.48; N 9.52; found: C 71.40, H 5.77, N 9.61

C4: Chromophore **S4** (152 mg, 0.35 mmol) and 2-(9*H*-carbazol-9-yl)acetic acid (118 mg, 0.525 mmol). The crude product was purified by column chromatography on silica gel (EtOAc/CHCl₃, 1:20 v/v) to afford a deep-red solid (202 mg, 89.9% yield). ¹H NMR (300 MHz, CDCl₃, 298 K): $\delta=1.82$ –1.91 (m, 4H; CH₂), 2.05 (s, 2H; C≡C–H), 2.27 (t, $J=6.6$ Hz, 4H; CH₂), 3.55 (t, $J=7.5$ Hz, 4H; NCH₂), 4.37 (t, $J=4.5$ Hz, 2H; OCH₂), 4.65 (t, $J=4.5$ Hz, 2H; COOCH₂), 6.74 (d, $J=9.0$ Hz, 2H; ArH), 7.16–7.34 (m, 6H; ArH), 7.75 (d, $J=8.7$ Hz, 1H; ArH), 7.82 (brs, 1H; ArH), 7.89 (d, $J=8.7$ Hz, 2H; ArH), 7.95 (d, $J=8.7$ Hz, 1H; ArH), 8.04 ppm (d, 2H; ArH); ¹³C NMR (75 MHz, CDCl₃, 298 K): $\delta=16.2$, 26.0, 44.9, 50.2, 63.5, 68.4, 69.8, 83.3, 108.5, 110.4, 111.7, 117.7, 119.9, 120.6, 123.4, 126.2, 126.7, 140.7, 144.6, 147.6, 148.1, 151.5, 154.8, 168.7 ppm; UV/Vis (THF, 1×10^{-5} mmol mL⁻¹): $\lambda_{\max}=493$ nm; IR (thin film): $\tilde{\nu}=3296$ (C≡C–H), 1715 (C=O), 1517, 1337 cm⁻¹ (NO₂); elemental analysis calcd (%) for C₃₈H₃₅N₅O₅: C 71.12; H 5.50; N 10.91; found: C 71.55, H 5.09, N 10.98.

C5: Chromophore **S4** (499.7 mg, 1.15 mmol) and pentafluorobenzoic acid (365.8 mg, 1.73 mmol). The crude product was purified by column chromatography on silica gel (EtOAc/CHCl₃, 1:20 v/v) to afford a deep-red solid (686.2 mg, 94.9% yield). ¹H NMR (400 MHz, CDCl₃, 298 K): δ = 1.87 (m, 4H; CH₂), 2.05 (s, 2H; C≡C-H), 2.30 (m, 4H; CH₂), 3.58 (t, *J* = 8.0 Hz, 4H; NCH₂), 4.56 (t, *J* = 4.0 Hz, 2H; OCH₂), 4.88 (t, *J* = 4.0 Hz, 2H; COOCH₂), 6.76 (d, *J* = 8.0 Hz, 2H; ArH), 7.69 (d, *J* = 8.0 Hz, 1H; ArH), 7.83 (d, *J* = 8.0 Hz, 2H; ArH), 7.94 ppm (m, 2H; ArH); ¹³C NMR (75 MHz, CDCl₃, 298 K): δ = 15.9, 25.7, 49.9, 64.2, 67.9, 69.4, 83.0, 110.2, 111.2, 117.5, 126.3, 144.1, 147.5, 147.8, 151.1, 154.4, 158.9 ppm; UV/Vis (THF, 1 × 10⁻⁵ mmol mL⁻¹): λ_{max} = 489 nm; IR (KBr): ν̄ = 3299 (C≡C-H), 1743 (C=O), 1516, 1336 cm⁻¹ (NO₂); elemental analysis calcd (%) for C₃₁H₂₅N₄O₅F₅: C 59.66; H 4.01; N 8.91; found: C 59.24, H 3.95, N 8.91.

Synthesis of Chromophore **S5**

N-Phenyldiethanolamine (1.08 g, 6.0 mmol), 4-iodobenzoic acid (4.46 g, 18.0 mmol), EDC (4.60 g, 24.0 mmol), and DMAP (288 mg, 2.40 mmol) were dissolved in dry CH₂Cl₂ (120 mL) and the mixture was stirred at RT for 3 days. Then, the mixture was treated with a saturated solution of citric acid, extracted with CH₂Cl₂, and washed with brine and a saturated solution of citric acid. After the removal of the solvent, the crude product was recrystallized from acetone to afford a white solid (3.80 g, 98.8% yield). ¹H NMR (300 MHz, [D₆]DMSO, 298 K): δ = 3.79 (t, *J* = 5.1 Hz, 4H; NCH₂), 4.41 (t, *J* = 5.1 Hz, 4H; OCH₂), 6.63 (t, *J* = 7.2 Hz, 1H; ArH), 6.88 (d, *J* = 8.4 Hz, 2H; ArH), 7.17 (t, *J* = 7.8 Hz, 2H; ArH), 7.63 (d, *J* = 8.1 Hz, 4H; ArH), 7.87 ppm (d, *J* = 8.1 Hz, 4H; ArH); ¹³C NMR (75 MHz, [D₆]DMSO, 298 K): δ = 50.4, 64.1, 103.6, 113.7, 117.9, 130.6, 130.8, 132.5, 139.3, 149.0, 167.1 ppm. MS (EI): *m/z*: 641.09 [M]⁺; calcd: 641.24.

Synthesis of Chromophore **C6**

Compound **S5** (641.2 mg, 1.0 mmol) and diazonium salt **S6** (284.0 mg, 1.0 mmol) were dissolved in DMF at 0°C and the reaction mixture was stirred for 12 h at 0°C. Then, the mixture was treated with water, extracted with CH₂Cl₂, and washed with brine. The organic layer was dried over anhydrous sodium sulfate. After removal of the organic solvent, the crude product was purified by column chromatography on silica gel (EtOAc/petroleum ether, 1:4 v/v) to afford a red solid (740 mg, 88.4% yield). ¹H NMR (400 MHz, CDCl₃, 298 K): δ = 1.30 (t, *J* = 8.0 Hz, 3H; CH₃), 3.16 (q, 8.0 Hz, 2H; SCH₂), 3.92 (t, *J* = 8.0 Hz, 4H; NCH₂), 4.55 (t, *J* = 8.0 Hz, 4H; COOCH₂), 6.95 (d, *J* = 8.0 Hz, 2H; ArH), 7.67 (d, *J* = 8.0 Hz, 4H; ArH), 7.79 (d, *J* = 8.0 Hz, 4H; ArH), 7.91 (d, *J* = 8.0 Hz, 2H; ArH), 7.96–8.02 ppm (m, 4H; ArH); ¹³C NMR (75 MHz, CDCl₃, 298 K): δ = 7.7, 49.9, 50.9, 62.2, 101.4, 112.2, 123.1, 126.2, 129.2, 129.5, 131.2, 138.1, 144.6, 151.0, 156.3, 166.2 ppm; UV/Vis (THF, 1 × 10⁻⁵ mmol mL⁻¹): λ_{max} = 430 nm; IR (KBr): ν̄ = 1716 (C=O), 1132 cm⁻¹ (SO₂); MS (EI): *m/z*: 837.83 [M]⁺; calcd: 837.46; elemental analysis calcd (%) for C₃₂H₂₉N₅O₆Si₂: C 45.89; H 3.49; N 5.02; found: C 46.02, H 3.63, N 5.18.

General Procedure for the Synthesis of Polymers **P1–P5**

A mixture of the nitro-based chromophore (**C1–C5**), sulfonyl-based chromophore **C6**, copper(I) iodide (5 mol %), triphenylphosphine (5 mol %), and [Pd(PPh₃)₄] (3 mol %) was carefully degassed and charged with argon. Then, THF (5 mL) and Et₃N (1 mL) were added and the reaction was stirred for 3.5 days at about 30°C. The mixture was passed through a cotton filter and dropped into a large volume of MeOH. The precipitate was collected, further purified by several precipitations of its solution in THF with acetone, and dried under vacuum at 40°C to a constant weight.

P1: Chromophore **C1** (74.9 mg, 0.20 mmol) and chromophore **C6** (167.5 mg, 0.20 mmol). Polymer **P1** was obtained as a red powder (141 mg, 73.8% yield). ¹H NMR (300 MHz, CDCl₃, 298 K): δ = 1.2–1.4 (CH₃), 1.4–1.8 (CH₂), 1.8–2.1 (CH₂), 2.4–2.6 (CH₂), 3.0–3.1 (SCH₂), 3.4–3.8 (NCH₂), 3.8–4.0 (OCH₂), 4.4–4.7 (COOCH₂), 6.7–7.0 (ArH), 7.2–7.6 (ArH), 7.6–8.0 (ArH), 8.2–8.4 ppm (ArH); ¹³C NMR (75 MHz, CDCl₃, 298 K): δ = 7.9, 17.4, 26.0, 26.3, 29.8, 50.0, 50.6, 51.1, 62.2, 81.4, 92.8, 111.9, 112.3, 123.0, 123.2, 125.0, 126.3, 126.6, 128.9, 129.6, 129.9, 131.9, 132.5, 138.5, 144.0, 144.6, 147.7, 151.2, 156.4, 157.0, 166.3 ppm; UV/Vis

(THF, 0.02 mg mL⁻¹): λ_{max} = 449 nm; IR (KBr): ν̄ = 2100 (C≡C), 1717 (C=O), 1513, 1335 (NO₂), 1137 cm⁻¹ (SO₂); GPC (polystyrene calibration): M_w = 9 900, M_w/M_n = 1.76.

P2: Chromophore **C2** (64.6 mg, 0.12 mmol) and chromophore **C6** (100.5 mg, 0.12 mmol). Polymer **P2** was obtained as a red powder (112 mg, 83.3% yield). ¹H NMR (400 MHz, CDCl₃, 298 K): δ = 1.2–1.4 (CH₃), 1.4–2.1 (CH₂), 2.4–2.6 (CH₂), 3.1–3.2 (SCH₂), 3.5–3.7 (NCH₂), 3.8–4.0 (OCH₂), 4.4–4.7 (COOCH₂), 4.8–4.9 (COOCH₂), 6.7–6.8 (ArH), 6.8–7.0 (ArH), 7.3–7.5 (ArH), 7.6–8.0 ppm (ArH); ¹³C NMR (75 MHz, CDCl₃, 298 K): δ = 7.7, 17.3, 26.3, 49.9, 50.5, 50.9, 62.1, 63.4, 68.9, 81.3, 92.7, 111.8, 112.2, 117.6, 123.1, 126.2, 126.6, 128.6, 128.8, 129.5, 129.8, 129.9, 131.8, 133.3, 138.1, 144.6, 148.2, 151.1, 155.2, 156.3, 166.1, 166.6 ppm; UV/Vis (THF, 0.02 mg mL⁻¹): λ_{max} = 448 nm; IR (KBr): ν̄ = 1716 (C=O), 1514, 1336 (NO₂), 1136 cm⁻¹ (SO₂); GPC (polystyrene calibration): M_w = 12 900, M_w/M_n = 1.56.

P3: Chromophore **C3** (53.0 mg, 0.09 mmol) and chromophore **C6** (75.3 mg, 0.09 mmol). Polymer **P3** was obtained as a red powder (94 mg, 89.3% yield). ¹H NMR (400 MHz, CDCl₃, 298 K): δ = 1.2–1.4 (CH₃), 1.8–2.1 (CH₂), 2.4–2.6 (CH₂), 3.0–3.1 (SCH₂), 3.4–3.7 (NCH₂), 3.8–4.0 (OCH₂), 4.4–4.7 (COOCH₂), 4.8–4.9 (COOCH₂), 6.6–6.7 (ArH), 6.8–7.0 (ArH), 7.2–7.6 (ArH), 7.6–8.1 (ArH), 8.8–8.9 ppm (ArH); ¹³C NMR (75 MHz, CDCl₃, 298 K): δ = 7.7, 17.3, 26.2, 44.8, 49.8, 50.4, 50.9, 62.1, 63.4, 68.2, 81.3, 92.8, 108.5, 112.1, 117.2, 119.9, 120.6, 123.1, 126.1, 126.7, 128.8, 128.8, 129.8, 131.8, 138.1, 140.6, 144.4, 151.0, 154.8, 156.3, 158.6, 160.6, 166.1 ppm; UV/Vis (THF, 0.02 mg mL⁻¹): λ_{max} = 450 nm; IR (KBr): ν̄ = 1716 (C=O), 1514, 1335 (NO₂), 1137 cm⁻¹ (SO₂); GPC (polystyrene calibration): M_w = 13 200, M_w/M_n = 1.70.

P4: Chromophore **C4** (57.8 mg, 0.09 mmol) and chromophore **C6** (75.3 mg, 0.09 mmol). Polymer **P4** was obtained as a red powder (98 mg, 89.1% yield). ¹H NMR (400 MHz, CDCl₃, 298 K): δ = 1.2–1.4 (CH₃), 1.8–2.0 (CH₂), 2.4–2.6 (CH₂), 3.0–3.2 (SCH₂), 3.4–3.8 (NCH₂), 3.8–4.0 (OCH₂), 4.2–4.4 (NCH₂), 4.4–4.7 (COOCH₂), 6.7–6.8 (ArH), 6.8–7.0 (ArH), 7.1–7.4 (ArH), 7.6–8.0 ppm (ArH); ¹³C NMR (75 MHz, CDCl₃, 298 K): δ = 7.7, 17.3, 26.3, 49.8, 50.4, 50.9, 62.0, 63.3, 68.7, 81.2, 92.7, 110.6, 111.7, 112.1, 117.5, 123.0, 124.7, 126.0, 126.2, 126.4, 126.6, 126.9, 128.0, 128.8, 129.5, 129.8, 130.8, 131.7, 133.7, 133.9, 138.3, 144.5, 148.2, 151.2, 155.0, 156.3, 166.1, 167.5 ppm; UV/Vis (THF, 0.02 mg mL⁻¹): λ_{max} = 451 nm; IR (KBr): ν̄ = 2100 (C≡C), 1716 (C=O), 1514, 1336 (NO₂), 1138 cm⁻¹ (SO₂); GPC (polystyrene calibration): M_w = 14 900, M_w/M_n = 1.99.

P5: Chromophore **C5** (75.4 mg, 0.12 mmol) and chromophore **C6** (100.5 mg, 0.12 mmol). Polymer **P5** was obtained as a red powder (116 mg, 79.8% yield). ¹H NMR (400 MHz, CDCl₃, 298 K): δ = 1.2–1.4 (CH₃), 1.8–2.1 (CH₂), 2.4–2.6 (CH₂), 3.1–3.2 (SCH₂), 3.5–3.7 (NCH₂), 3.8–4.0 (OCH₂), 4.4–4.7 (COOCH₂), 4.7–4.8 (COOCH₂), 6.6–6.7 (ArH), 6.8–7.1 (ArH), 7.2–7.6 (ArH), 7.6–8.2 ppm (ArH); ¹³C NMR (75 MHz, CDCl₃, 298 K): δ = 7.37, 17.0, 25.9, 49.6, 50.2, 50.6, 61.8, 64.2, 68.0, 80.9, 92.4, 110.4, 111.4, 111.9, 117.5, 122.7, 125.9, 126.2, 128.5, 129.1, 129.4, 130.9, 131.4, 137.8, 138.1, 144.2, 147.5, 147.9, 150.9, 154.4, 156.1, 158.8, 165.8 ppm; UV/Vis (THF, 0.02 mg mL⁻¹): λ_{max} = 449 nm; IR (KBr): ν̄ = 2100 (C≡C), 1718 (C=O), 1515, 1334 (NO₂), 1138 cm⁻¹ (SO₂); GPC (polystyrene calibration): M_w = 13 800, M_w/M_n = 1.61.

Preparation of Polymer Thin Films

The polymers were dissolved in THF (concentration: about 4 wt. %), and the solutions were filtered through syringe filters. The polymer films were spin-coated onto indium tin oxide (ITO)-coated glass substrates, which were sequentially cleaned with DMF, acetone, distilled water, and THF again in an ultrasound bath before use. Residual solvent was removed by heating the films in a vacuum oven at 40°C.

NLO Measurements of the Poled Films

The second-order optical nonlinearity of the polymers was determined by in situ second harmonic generation (SHG) experiments in a closed temperature-controlled oven with optical windows and three needle electrodes. The films were kept at 45° to the incident beam and poled inside the oven and the SHG intensity was monitored simultaneously. The poling conditions were as follows: Temperature: different for each polymer

(Table 3); voltage: 7.5 kV at the needle point; gap distance: 0.8 cm. The SHG measurements were carried out with a Nd:YAG laser that was operating at a 10 Hz repetition rate and an 8 ns pulse width at 1064 nm. A Y-cut quartz crystal was used as a reference.

Acknowledgements

We are grateful to the National Science Foundation of China (21034006) for financial support.

- [1] a) D. M. Burland, R. D. Miller, C. A. Walsh, *Chem. Rev.* **1994**, *94*, 31–75; b) Y. Bai, N. Song, J. P. Gao, X. Sun, X. Wang, G. Yu, Z. Y. Wang, *J. Am. Chem. Soc.* **2005**, *127*, 2060–2621; c) T. J. Marks, M. A. Ratner, *Angew. Chem.* **1995**, *107*, 167–187; *Angew. Chem. Int. Ed. Engl.* **1995**, *34*, 155–173; d) D. Yu, A. Gharavi, L. P. Yu, *J. Am. Chem. Soc.* **1995**, *117*, 11680–11686; e) S. R. Marder, B. Kippelen, A. K. Y. Jen, N. Peyghambarian, *Nature* **1997**, *388*, 845–851; f) M. Lee, H. E. Katz, C. Erben, D. M. Gill, P. Gopalan, J. D. Heber, D. J. McGee, *Science* **2002**, *298*, 1401–1403; g) Y. Shi, C. Zhang, H. Zhang, J. H. Bechtel, L. R. Dalton, B. H. Robinson, W. H. Steier, L. R. Dalton, *Science* **2000**, *288*, 119–122; h) C. V. Mclaughlin, M. Hayden, B. Polishak, S. Huang, J. D. Luo, T.-D. Kim, A. K. Y. Jen, *Appl. Phys. Lett.* **2008**, *92*, 151107–151109; i) L. R. Dalton, P. A. Sullivan, D. H. Bale, *Chem. Rev.* **2010**, *110*, 25–55; j) J. D. Luo, X. H. Zhou, A. K. Y. Jen, *J. Mater. Chem.* **2009**, *19*, 7410–7424; k) J. D. Luo, S. Huang, Z. W. Shi, B. M. Polishak, X. H. Zhou, A. K. Y. Jen, *Chem. Mater.* **2011**, *23*, 544–553; l) J. Wu, S. Bo, J. Liu, T. Zhou, H. Xiao, L. Qiu, Z. Zhen, X. Liu, *Chem. Commun.* **2012**, *48*, 9637–9639.
- [2] a) M. A. Mortazavi, A. Knoesen, S. T. Kowel, B. G. Higgins, A. Dienes, *J. Opt. Soc. Am. B* **1989**, *6*, 733–741; b) K. D. Singer, M. G. Kuzyk, W. R. Holland, J. E. Sohn, S. J. Lalama, *Appl. Phys. Lett.* **1988**, *53*, 1800–1802; c) K. D. Singer, J. E. Sohn, S. J. Lalama, *Appl. Phys. Lett.* **1986**, *49*, 248–250.
- [3] a) B. H. Robinson, L. R. Dalton, *J. Phys. Chem. A* **2000**, *104*, 4785–4795; b) B. H. Robinson, L. R. Dalton, H. W. Harper, A. Ren, F. Wang, C. Zhang, G. Todorova, M. Lee, R. Aniszfeld, S. Garner, A. Chen, W. H. Steier, S. Houbrecht, A. Persoons, I. Ledoux, J. Zyss, A. K.-Y. Jen, *Chem. Phys.* **1999**, *245*, 35–50; c) D. R. Kanis, M. A. Ratner, T. J. Marks, *Chem. Rev.* **1994**, *94*, 195.
- [4] a) M. J. Cho, D. H. Choia, P. A. Sullivan, A. J.-P. Akelaitis, L. R. Dalton, *Prog. Polym. Sci.* **2008**, *33*, 1013–1058; b) Y. V. Pereverzev, K. N. Gunnerson, O. V. Prezhdo, P. A. Sullivan, Y. Liao, B. C. Olbricht, A. J. P. Akelaitis, A. K.-Y. Jen, L. R. Dalton, *J. Phys. Chem. C* **2008**, *112*, 4355–4363; c) H. Ma, S. Liu, J. Luo, S. Suresh, L. Liu, S. H. Kang, M. Haller, T. Sassa, L. R. Dalton, A. K. Y. Jen, *Adv. Funct. Mater.* **2002**, *12*, 565–574; d) Z. Shi, J. Luo, S. Huang, X.-H. Zhou, T.-D. Kim, Y.-J. Cheng, B. M. Polishak, T. R. Younkin, B. A. Block, A. K.-Y. Jen, *Chem. Mater.* **2008**, *20*, 6372–6377.
- [5] L. R. Dalton, W. H. Steier, B. H. Robinson, C. Zhang, A. Ren, S. Garner, A. Chen, T. Londergan, L. Irwin, B. Carlson, L. Fifield, G. Phelan, C. Kincaid, J. Amend, A. K.-Y. Jen, *J. Mater. Chem.* **1999**, *9*, 1905–1920.
- [6] a) Z. Li, Z. Li, C. Di, Z. Zhu, Q. Li, Q. Zeng, K. Zhang, Y. Liu, C. Ye, J. Qin, *Macromolecules* **2006**, *39*, 6951–6961; b) Q. Zeng, Z. Li, Z. Li, C. Ye, J. Qin, B. Z. Tang, *Macromolecules* **2007**, *40*, 5634–5637; c) Q. Li, Z. Li, F. Zeng, W. Gong, Z. Li, Z. Zhu, Q. Zeng, S. Yu, C. Ye, J. Qin, *J. Phys. Chem. B* **2007**, *111*, 508–514; d) Z. Li, P. Li, S. Dong, Z. Zhu, Q. Li, Q. Zeng, Z. Li, C. Ye, J. Qin, *Polymer* **2007**, *48*, 3650–3657; e) Z. Li, S. Dong, G. Yu, Z. Li, Y. Liu, C. Ye, J. Qin, *Polymer* **2007**, *48*, 5520–5529; f) Z. Li, S. Dong, P. Li, Z. Li, C. Ye, J. Qin, *J. Polym. Sci. Part A* **2008**, *46*, 2983–2993; g) Z. Li, Q. Li, J. Qin, *Polym. Chem.* **2011**, *2*, 2723–2740; h) Q. Li, C. Lu, J. Zhu, E. Fu, C. Zhong, S. Li, Y. Cui, J. Qin, Z. Li, *J. Phys. Chem. B* **2008**, *112*, 4545–4551; i) Q. Li, Z. Li, C. Ye, J. Qin, Z. Li, *J. Phys. Chem. B* **2008**, *112*, 4928–4933; j) Z. Li, G. Qiu, C. Ye, J. Qin, Z. Li, *Dyes Pigm.* **2012**, *94*, 16–22.
- [7] a) Z. Li, G. Yu, W. Wu, Y. Liu, C. Ye, J. Qin, Z. Li, *Macromolecules* **2009**, *42*, 3864–3868; b) Z. Li, W. Wu, Q. Li, G. Yu, L. Xiao, Y. Liu, C. Ye, J. Qin, Z. Li, *Angew. Chem.* **2010**, *122*, 2823–2827; *Angew. Chem. Int. Ed.* **2010**, *49*, 2763–2767; c) W. Wu, L. Huang, C. Song, G. Yu, C. Ye, Y. Liu, J. Qin, Q. Li, Z. Li, *Chem. Sci.* **2012**, *3*, 1256–1261.
- [8] a) W. Wu, C. Ye, G. Yu, Y. Liu, J. Qin, Z. Li, *Chem. Eur. J.* **2012**, *18*, 4426–4434; b) W. Wu, C. Li, G. Yu, Y. Liu, C. Ye, J. Qin, Z. Li, *Chem. Eur. J.* **2012**, *18*, 11019–11028; c) W. Wu, L. Huang, L. Xiao, Q. Huang, R. Tang, C. Ye, J. Qin, Z. Li, *RSC Adv.* **2012**, *2*, 6520–6526; d) W. Wu, C. Wang, C. Zhong, C. Ye, G. Qiu, J. Qin, Z. Li, *Polym. Chem.* **2013**, *4*, 378–386.
- [9] a) C. R. Patrick, G. S. Prosser, *Nature* **1960**, *187*, 1021; b) G. W. Coates, A. R. Dunn, L. M. Henling, D. A. Dougherty, R. H. Gubbs, *Angew. Chem.* **1997**, *109*, 290–293; *Angew. Chem. Int. Ed. Engl.* **1997**, *36*, 248–251.
- [10] a) T. D. Kim, J. Kang, J. Luo, S. Jang, J. Na, N. Tucker, J. B. Benedict, L. R. Dalton, T. Gray, R. M. Overney, D. H. Park, W. N. Herman, A. K.-Y. Jen, *J. Am. Chem. Soc.* **2007**, *129*, 488–489; b) X. Zhou, J. Luo, S. Huang, T. Kim, Z. Shi, Y. Cheng, S. Jang, D. B. Knorr, R. M. Overney, A. K.-Y. Jen, *Adv. Mater.* **2009**, *21*, 1976–1981.
- [11] a) W. Wu, Q. Huang, G. Qiu, C. Ye, J. Qin, Z. Li, *J. Mater. Chem.* **2012**, *22*, 18486–18495; b) W. Wu, Y. Fu, C. Wang, C. Ye, J. Qin, Z. Li, *Chem. Asian J.* **2011**, *6*, 2787–2795; c) W. Wu, C. Wang, R. Tang, Y. Fu, C. Ye, J. Qin, Z. Li, *J. Mater. Chem. C* **2013**, *1*, 717–728; d) W. Wu, G. Yu, Y. Liu, C. Ye, J. Qin, Z. Li, *Chem. Eur. J.* **2013**, *19*, 630–641; e) W. Wu, Z. Zhu, G. Qiu, C. Ye, J. Qin, Z. Li, *J. Polym. Sci. Part A* **2012**, *50*, 5124–5133.
- [12] a) Z. Li, J. Qin, S. Li, C. Ye, J. Luo, Y. Cao, *Macromolecules* **2002**, *35*, 9232–9235; b) Z. Li, J. Li, J. Qin, A. Qin, C. Ye, *Polymer* **2005**, *46*, 363–368; c) Z. Li, W. Gong, J. Qin, Z. Yang, C. Ye, *Polymer* **2005**, *46*, 4971–4978; d) Z. Li, J. Hua, Q. Li, C. Huang, A. Qin, C. Ye, J. Qin, *Polymer* **2005**, *46*, 11940–11948; e) Z. Li, C. Huang, J. Hua, J. Qin, Z. Yang, C. Ye, *Macromolecules* **2004**, *37*, 371–376.
- [13] M. Kauranen, T. Verbiest, C. Boutton, M. N. Teeren, K. Clays, A. J. Schouten, R. J. M. Nolte, A. Persoons, *Science* **1995**, *270*, 966–969.
- [14] a) Z. Li, W. Wu, C. Ye, J. Qin, Z. Li, *Polymer* **2012**, *53*, 153–160; b) Y. Tian, X. Zhang, J. Wu, H. Fun, M. Jiang, Z. Xu, *New J. Chem.* **2002**, *26*, 1468–1473.

Received: January 4, 2013
Published online: ■ ■ ■, 0000

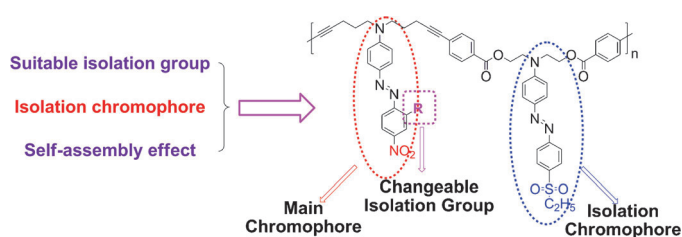
FULL PAPER

Nonlinear Optics

Wenbo Wu, Cheng Ye, Jingui Qin,
Zhen Li* —————



Further Enhancement of the Second-Order Nonlinear Optical (NLO) Coefficient and the Stability of NLO Polymers that Contain Isolation Chromophore Moieties by Using the “Suitable Isolation Group” Concept and the Ar/Ar^F Self-Assembly Effect



Second the best: Second-order NLO poly(arylene-ethynylene)s that contained an isolation chromophore were obtained, in which the isolation groups

were introduced by using the “suitable isolation group” concept or the Ar–Ar^F self-assembly effect.